Balanced nonstationary turbulence

Konstantinos Steiros*
Department of Aeronautics, Imperial College London, SW7 2AZ London, United Kingdom

(Received 1 November 2021; accepted 4 March 2022; published 23 March 2022)

Kolmogorov's 1941 (K41) framework remains central to the understanding of turbulent flows. However, in unsteady turbulence, K41's critical equilibrium assumption is expected to hold in an asymptotic manner, as the Reynolds number and wave numbers tend to infinity, rendering K41 not strictly valid at finite wave numbers. This work proposes a generalization of K41 for out-of-equilibrium effects and cascades far from initial conditions. The main result is a correction to the $-5/3$ law for out-of-equilibrium eddies, unrelated to intermittency effects. Experimental and numerical evidence is provided in support of the theoretical results.

DOI: 10.1103/PhysRevE.105.035109

I. INTRODUCTION

A landmark of out-of-equilibrium physics is Kolmogorov's 1941 (K41) phenomenological theory of turbulence [1–3]. Its predictions regulate many quantities of engineering interest, while it is the basis of most turbulence models currently used in science and engineering. In this framework, turbulence is depicted as a cascade of energy, moving, on average, from large inviscid flow scales to small dissipative ones, where it is converted into heat [4–6]. In between, an intermediate range of scales, whose properties are not affected by either viscous effects or large-scale phenomena, is formed. K41 produces several predictions for this intermediate range and, by extension, for turbulence as a whole. These predictions have been validated in a variety of flows, giving strong credibility to the theory.

A cornerstone assumption of the K41 theory is that of cascade equilibrium (see the chapter on "The Universal Equilibrium Theory" in Batchelor [6]). Equilibrium is used here in the context of stationarity and not in that of thermodynamic equilibrium encountered in statistical physics. Hence, in unsteady flow regimes, the entirety of the cascade cannot be expected to be in equilibrium, which is approached only as turbulent eddies become vanishingly small and the Reynolds number becomes infinite [4,7]. For such unsteady cascades K41 is therefore an asymptotic limit and cannot be expected to exactly describe finite, out-of-equilibrium wave numbers, the physics of which remain obscure.

The recent observations of Goto and Vassilicos [8] have shown that out-of-equilibrium eddies exhibit collective dynamics, at least in certain flow cases. Such observations raise hopes for an out-of-equilibrium theory of turbulence. In particular, it was observed that, far from initial conditions, a portion of a freely decaying homogeneous turbulence cascade reaches a "balanced" nonequilibrium state where the terms of the budget equation scale with each other. The possibility of an asymptotic approach to a balanced energy budget far from initial conditions was previously postulated by George [9,10] for the whole spectral range. Goto and Vassilicos observed it for eddies close to the integral length scale of the cascade. We note that this balance leads to the establishment of Kolmogorov's dissipation scaling [8,11].

Based on the above observations, this paper proposes an extension of K41 for out-of-equilibrium phenomena in quasi-isotropic eddies and for cascades sufficiently far from the initial conditions. It is first shown that Goto and Vassilicos's observation of "balance" implies a self-preserving interscale energy flux. Combining that result with the assumption of simple transportation of energy along the cascade leads to a correction to the $-5/3$ law for out-of-equilibrium effects. In agreement with K41, this correction becomes asymptotically negligible, as the Reynolds number becomes infinite and the eddy size tends to zero. It is noted that this correction is not relevant for intermittency effects, e.g., the OK62 theory of Oboukhov and Kolmogorov [12,13]. Additionally, the revised framework yields a link between the K41 phenomenology and the dissipation equation of the $k-\epsilon$ model for homogeneous decaying turbulence [14]. The assumptions and conclusions of this work are validated using data from laboratory and numerical experiments.

II. THE EQUILIBRIUM ASSUMPTION

We first review the equilibrium assumption of the K41 framework in spectral space (see also [15]). Consider homogeneous decaying turbulence, a common test bench for turbulence theories. This can be achieved experimentally using a turbulence grid in a wind tunnel or numerically by simulating turbulence in a periodic box. This work's assumptions and conclusions are validated using both techniques. Details on the methodology can be found in Appendix A.

In spectral space, homogeneous decaying turbulence can be described by the interscale energy budget

$$\frac{\partial K^{>}(k,t)}{\partial t} = \Pi(k,t) - \epsilon^{>}(k,t), \tag{1}$$

*k.steiros13@imperial.ac.uk

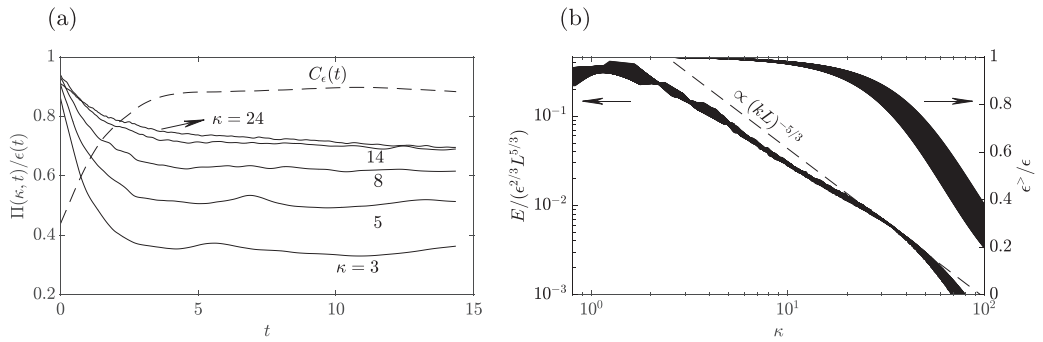

FIG. 1. (a) Π/ϵ over time for the DNS data set (see Appendix A for numerical details), evaluated at various normalized wave numbers $\kappa = kL$ (at $t = 0$ the forcing stops). $\Pi/\epsilon = 1$, which marks Kolmogorov's equilibrium, is not fulfilled at any normalized wave number when C_ϵ (dashed line) is constant. (b) Normalized energy spectrum and high-pass dissipation for $t > 3.3$.

where $K^>(k,t) = \int_k^\infty E(k,t)dk$ and $\epsilon^>(k,t) = \int_k^\infty k^2 E(k,t)dk$ are the high-pass-filtered turbulence kinetic energy and dissipation rate, respectively, with $E(k,t)$ being the energy spectrum. $\Pi(k,t)$ is the interscale flux from wave numbers smaller than k to wave numbers larger than k. Kolmogorov's equilibrium assumption states that for sufficiently large Reynolds numbers and for eddies which are of negligible size compared to the large scales of the flow, the cascade is approximately stationary, i.e., $\frac{\partial K^>}{\partial t} \approx 0$ [1,4,16]. If we also consider scales which are far from dissipative phenomena, i.e., $k\eta \to 0$, with $\eta = (\nu^3/\epsilon)^{1/4}$, then viscous effects can be neglected, and thus, $\epsilon^>(k,t) \approx \epsilon(t)$, with $\epsilon(t) = \int_0^\infty k^2 E(k,t)dk$ being the total dissipation of the cascade. Given the above, Eq. (1) reduces to

$$\Pi(k,t) \approx \epsilon(t). \tag{2}$$

The above expression of the equilibrium assumption has two important repercussions. First, we note that the interscale energy flux $\Pi(k,t)$ is expected to scale as $K(t)^{3/2}/L(t)$ for $kL \approx 1$ [15]. Therefore, extension of Eq. (2) up to $kL \approx 1$ readily leads to the Kolmogorov dissipation scaling $\epsilon(t) \approx C_\epsilon[2K(t)/3]^{3/2}/L(t)$, with C_ϵ being constant. Second, the combination of the dimensional analysis result $E(k,t) \propto \Pi(k,t)^{2/3}k^{-5/3}$ with expression (2) yields the relation $E(k,t) \propto \epsilon^{2/3}k^{-5/3}$, which is Kolmogorov's $-5/3$ law [4].

We note that exact equilibrium in an unsteady cascade [and thus an exact equality in Eq. (2)] can be expected only asymptotically, i.e., when $\mathrm{Re} \to \infty$ and $kL \to \infty$, where $L(t) = \frac{3\pi}{4}\int_0^\infty k^{-1}E(k,t)dk/K(t)$ is the integral length scale of the flow [$K(t) = \int_0^\infty E(k,t)dk$ is the total kinetic energy of the cascade]. A natural problem then is to determine the mathematical expression for this asymptotic behavior for a given flow.

III. BALANCED CASCADE

The recent observations of Goto and Vassilicos [8] imply a certain asymptotic expression for the interscale energy flux for decaying turbulence, sufficiently far from initial conditions. In particular, Goto and Vassilicos noted that, due to the asymptotic approach of equilibrium in an unsteady cascade, $\frac{\partial K^>}{\partial t}$ will not be exactly zero when $\kappa = kL$ is of finite magnitude, and at small κ it may assume values which are comparable to those of the other terms of the budget equation (1) (see Ref. [8]). Hence, the expression $\Pi(k,t) \approx \epsilon(t)$ cannot be extended to $\kappa \approx 1$, and the Kolmogorov dissipation scaling $C_\epsilon = \text{const}$ cannot be ensured. For instance, for decaying cascades sufficiently close to initial conditions C_ϵ has been found to be nonconstant and instead follows reproducible non-Kolmogorov scalings [8,16].

Nevertheless, far from initial conditions, decaying homogeneous cascades have long been known to be characterized by $C_\epsilon = \text{const}$. For instance, in the periodic box results used in this study $C_\epsilon = \text{const}$ is observed at 3.5-dimensional time units (corresponding to approximately three turnover times) after the forcing stops (see Fig. 1(a) and Appendix A; see also Ref. [17]). In grid turbulence experiments the transition from nonconstant to constant C_ϵ occurs at a location 10 to 15 mesh sizes downstream of the grid (see [11] and Appendix A). The question then is how $C_\epsilon = \text{const}$ is achieved, despite the lack of equilibrium at the low wave numbers of the cascade.

As Goto and Vassilicos [8] observed, the above is possible because a particular organization of the out-of-equilibrium eddies occurs far from initial conditions. In particular, the terms of the budget equation (1) eventually become balanced, in the sense that they remain a fixed proportion of each other over time at $kL \approx 1$, a fact which explains the establishment of the classical dissipation scaling. Extending Goto and Vassilicos's observation, here we assume that, far from initial conditions, a decaying cascade eventually reaches an asymptotic balanced state, where the terms of the budget equation evolve together beyond a critical wave number. Expressed as symbols,

$$\frac{\partial K^>(\kappa,t)}{\partial t} \propto \Pi(\kappa,t) \propto \epsilon^>(\kappa,t) \tag{3}$$

for $\kappa > \kappa_c$. Similar cases of balance were previously postulated to characterize many other flow systems "far" from initial conditions, i.e., when initial transient modes have decayed [9].

We consider scales much larger than the dissipative ones, i.e., $k\eta \to 0$, and thus, $\epsilon^>(t) \approx \epsilon(t)$. Expression (3) then leads to the self-preserving expression

$$\Pi(\kappa,t) = \epsilon(t)g(\kappa), \tag{4}$$

where g is expected to be an increasing function, asymptotically tending to unity as both Re and kL tend to infinity, in

agreement with Kolmogorov's equilibrium assumption. Equation (4) is hence a candidate for expressing the asymptotic approach to Kolmogorov's equilibrium for cascades far from initial conditions, i.e., when initial transients have died.

In Fig. 1(a) we validate expression (4) using the periodic box direct numerical simulations (DNS) data. The DNS results support the above postulations, up to a point. Equation (4) is indeed valid for a variety of wave numbers larger than $\kappa_c = 3$ and when $t > 3.5$ (i.e., when $C_\epsilon = \text{const}$), while g is an increasing function of $\kappa = kL$, as per our postulation. However, g never reaches unity (equilibrium) and instead peaks at a maximum value of 0.73, after which it plateaus and even decreases. The end of the increase in g occurs approximately at those wave numbers where viscous effects start becoming important [i.e., $\epsilon^>$ becomes notably smaller than ϵ; see Fig. 1(b)]. Approximate equilibrium is therefore never reached in the DNS due to the latter's limited Reynolds number (Re_λ of approximately 150; see Appendix A). We expect that for simulations of higher Reynolds numbers the function g would continue increasing with kL, eventually reaching values very close to unity (i.e., equilibrium). The forced DNS of Ref. [18] and the Eddy damped quasi-normal markovian (EDQNM) simulations of Ref. [19] support this postulation.

Hence, the self-preserving expression (4) indeed seems to describe the approach to equilibrium of the nonequilibrium eddies of the periodic box data set after some time has passed since the end of the forcing. We now argue that this behavior induces a correction to the $-5/3$ law at quasi-isotropic eddies. The $-5/3$ law is derived on the basis of dimensional arguments [4] which yield the relationship $\frac{E(k,t)}{\Pi(k,t)^{2/3}L(t)^{5/3}} \propto \kappa^{-5/3}$. We retain this expression by assuming quasi-isotropy. Figure 7 in Appendix A indeed shows that the above relationship yields an excellent collapse of the DNS spectra for $kL > 2$. Using the above result in conjunction with Eq. (4), we obtain the following expression for $E(k,t)$:

$$\frac{E(k,t)}{\epsilon(t)^{2/3}L(t)^{5/3}} = C_k g(\kappa)^{2/3}\kappa^{-5/3}, \tag{5}$$

where C_k is a coefficient of proportionality which is postulated to be universal [20]. Equation (5) shows that, when equilibrium is not exact, we might expect a spectral slope different from $-5/3$, the latter being approached only as $g \to 1$ (equilibrium). In particular, since g is an increasing function of κ [see Fig. 1(a)] the slope of nonequilibrium eddies should be flatter than $-5/3$. Figure 1(b) shows that while the spectral slope of the DNS data set is quite close to the $-5/3$ prediction, it is indeed somewhat flatter than that. In the following sections we perform a more thorough assessment of the spectral slope, provide an expression for the function g, and validate these results with data from laboratory and numerical experiments.

IV. ANALYSIS AND RESULTS

A. Simple transportation of energy

Following Lumley [5], we expect that, at sufficiently high Reynolds numbers, a range of scales will form in the cascade, where effects linked to production or dissipation of turbulence kinetic energy will be negligible. Consequently, the energy there is conserved, simply transported downwards in the cascade. We interpret the above statement as the material derivative of the energy flux being zero in the self-preserving coordinate system of independent variables (κ, t):

$$D\Pi/Dt = \partial\Pi/\partial t + V\,\partial\Pi/\partial\kappa = 0\,. \tag{6}$$

Equation (6) poses a constraint which can be used to calculate the function g [see Eq. (5)], but to do that, we first need an expression for the interscale energy speed $V = d\kappa/dt$. Following the analysis of Pao [21], we expect that $dk/dt = C_v\Pi^{1/3}k^{5/3}$, where C_v is a coefficient of proportionality (note that Pao assumed C_v is equal to the inverse of the Kolmogorov constant, but here we allow it to take, more generally, an arbitrary value). Using equation (4) and the Kolmogorov dissipation scaling $\epsilon = C_\epsilon(\frac{2}{3}K)^{3/2}/L$, we end up with

$$dk/dt = \frac{3}{2}\frac{C_v}{C_\epsilon^{2/3}}\frac{\epsilon(t)}{L(t)K(t)}g(\kappa)^{1/3}\kappa^{5/3}.$$

The speed of the energy flux across normalized wave numbers is $\frac{d\kappa}{dt} = L\frac{dk}{dt} + k\frac{dL}{dt}$. We expect that the second term on the right hand side will be negligible compared to the first, i.e., $\frac{d\kappa}{dt} \approx L\frac{dk}{dt}$. That is because the timescale of the nonlinear energy transport of an individual eddy must be much smaller than that of the dilation of the entire cascade. This postulation was verified using the DNS data, and the term $k\frac{dL}{dt}$ was found to be at least an order of magnitude smaller than $L\frac{dk}{dt}$ after $\kappa = 2$ ($\frac{dk}{dt}$ was calculated using Pao's formula given above). Therefore, the spectral velocity is given by

$$V \approx \frac{3}{2}\frac{C_v}{C_\epsilon^{2/3}}\frac{\epsilon(t)}{K(t)}g(\kappa)^{1/3}\kappa^{5/3}. \tag{7}$$

Combining this result with Eqs. (4) and (6), we obtain

$$\frac{K}{\epsilon^2}\frac{d\epsilon}{dt} = -\frac{3}{2}\frac{C_v}{C_\epsilon^{2/3}}\frac{g'}{g^{2/3}}\kappa^{5/3} = -C_0, \tag{8}$$

where $g' = dg/d\kappa$. The left-hand side of Eq. (8) is a function of only time, while the right-hand side is a function of only the normalized wave number κ. Thus, both sides must equal a constant C_0, which is expected to depend only on initial conditions. In Fig. 2 we validate the above result with the DNS data

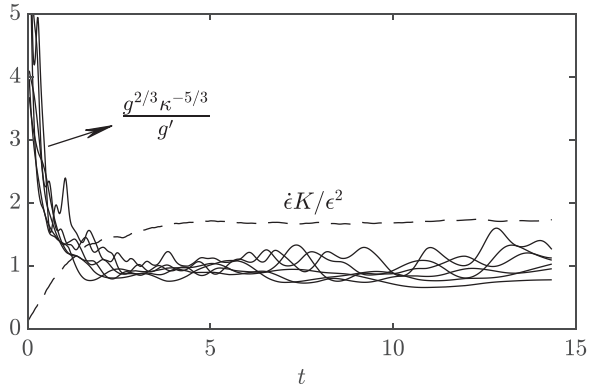

FIG. 2. Evolution of the two sides of Eq. (8) over time, using the DNS data set. $g^{2/3}\kappa^{-5/3}/g'$ (solid lines) is plotted for $\kappa = 3, 4, 5, 6, 7, 8, 10$.

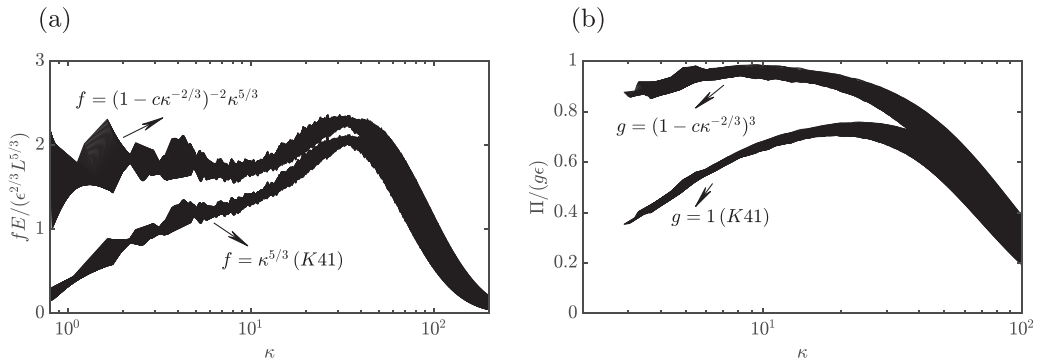

FIG. 3. Validation of expressions (11) and (12) using the DNS data. (a) Energy spectrum and (b) interscale energy flux for many time instances for $t > 3.3$. In both plots the curves are not flat using the K41 compensation and become flatter when using the proposed corrections of expressions (11) and (12), with the calculated value $c = 0.53$. f and g are as defined in the plots.

[note that $g(\kappa) \equiv \Pi(\kappa, t)/\epsilon(t)$]. Once the balanced cascade assumption becomes valid ($t > 3.5$; see Fig. 1), both sides of the equation become relatively constant, independent of time or wave number. We note that the collapse of $g^{2/3}\kappa^{-5/3}/g'$ is relatively good in the DNS for wave numbers smaller than $\kappa = 13$, i.e., smaller than the point where dissipative effects start becoming significant [see Fig. 1(b)].

B. Dissipation equation of the $k - \epsilon$ model

The left-hand side of Eq. (8) is

$$\frac{d\epsilon}{dt} = -C_0\frac{\epsilon^2}{K}, \tag{9}$$

which resembles the dissipation equation of the $k - \epsilon$ turbulence model for homogeneous decaying turbulence [4,14]. Using $\epsilon = -dK/dt$ and integrating, we find a power law decay for the kinetic energy without the need to assume turbulence invariants (see also [4]):

$$K = K_0\left(\frac{t}{t_0}\right)^{-\frac{1}{C_0 - 1}}, \tag{10}$$

with K_0 and t_0 being constants. If we do assume a turbulence invariant, we may calculate the constant C_0. Loitsyanskii's invariant yields $C_0 = 1.7$ [22], which is the value of the current DNS data set. It is noteworthy that non-Kolmogorov theories which assume a single characteristic length scale in turbulence (see, for instance, [10]) also lead to Eqs. (9) and (10), without the need to assume invariants. Here we show that these results can also be obtained from variants of the K41 theory.

C. A correction to the $-5/3$ law

By separating the variables on the right-hand side of Eq. (8) and integrating, we obtain $g = [1 - \frac{C_0 C_\epsilon^{2/3}}{3C_v}\kappa^{-2/3}]^3$, where the constant of integration was calculated using the fact that we expect equilibrium, i.e., $g \to 1$, as $\kappa \to \infty$ and $\mathrm{Re} \to \infty$. Expressions (4) and (5) then lead to

$$\frac{E(\kappa, t)}{\epsilon(t)^{2/3}L(t)^{5/3}} \approx C_k[1 - c\kappa^{-2/3}]^2\kappa^{-5/3}, \tag{11}$$

$$g(\kappa) \equiv \frac{\Pi(\kappa, t)}{\epsilon(t)} \approx [1 - c\kappa^{-2/3}]^3, \tag{12}$$

with $c = \frac{C_0 C_\epsilon^{2/3}}{3C_v}$ for $kL > \kappa_c$ and $k\eta \to 0$ at $Re \gg 1$ (but not necessarily tending to infinity). Determination of the constant c requires knowledge of C_ϵ, C_v, and C_0. However, only the latter can be calculated analytically, by assuming a turbulence invariant, as shown in the previous section. Thus, C_v and C_ϵ need to be determined from observations. From Figs. 1(a) and 2 we obtain $C_\epsilon \approx 0.9$ and $C_v \approx 1$ for the DNS, which lead to $c = 0.53$.

In Fig. 3 we validate the above expressions using the DNS data set, on lin-log axes. When plotted using Kolmogorov's compensation [$E\kappa^{5/3}/(\epsilon^{2/3}L^{5/3})$; see Fig. 3(a)], the energy spectrum curves collapse for different times but are nonconstant. A very small peak appears only at $\kappa \approx 40$, but this can be argued to be well inside the dissipative range [i.e., $\epsilon^{>}/\epsilon$ is far from unity; see Fig. 1(b)]. This nonconstancy is an indication that the $-5/3$ law is not exact in our range of scales. Expression (11), on the other hand, does make the compensated spectrum approximately constant up to $\kappa \approx 15$ [where dissipative phenomena start becoming important; see Fig. 1(b)]. Due to this constancy we may also calculate the value of the constant $C_k \approx 1.7$, close to documented values [18,20].

Figure 3(b) shows that the prediction of the equilibrium assumption $\Pi/\epsilon \approx 1$ [i.e., Eq. (2)] is not fulfilled at any wave number of the DNS data set. Instead, Π/ϵ is an increasing function of κ until approximately $\kappa = 20$, where it assumes its maximum values and then drops, as dissipative phenomena become important [see Fig. 1(b)]. The proposed compensated energy flux renders the interscale flux relatively constant, with a value very close to unity for $\kappa < 20$, in agreement with expression (12). We reiterate that for simulations with higher Reynolds numbers, the onset of dissipative effects would be delayed to larger normalized wave numbers, and we would expect a continually increasing Π/ϵ until it reached approximately a value of unity at wave numbers where nonequilibrium effects would be negligible. After that point, until dissipative phenomena started appearing, the $-5/3$ law would become almost exact, in accordance with K41 (see, for instance, [18]).

We now ascertain whether the trends found in the numerical simulation are also observed in hot-wire measurements of grid turbulence. However, the above results are derived for the

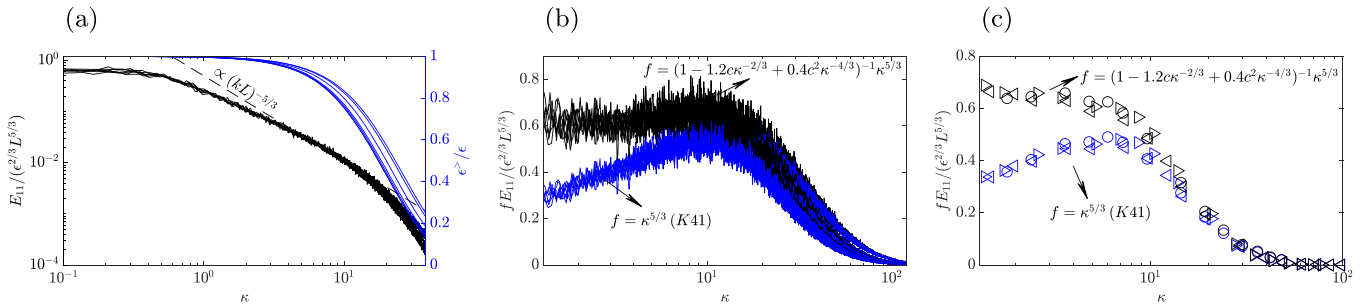

FIG. 4. (a) Measured normalized 1D energy spectrum and high-pass dissipation of the G1 grid at seven measurement stations where $C_\epsilon \approx 1.1$ and Re_λ is varied from 129 to 94. (b) Validation of expression (13) using the same grid-turbulence data set, with the calculated value $c = 0.65$. (c) Compensated 1D spectra from the 2-in. grid of Comte-Bellot and Corrsin [24]. The three different symbols represent different locations downstream from the grid (Re_λ varies between 60 and 72, and C_ϵ remains constant) while $c = 0.63$. f is as defined in the plots.

three-dimensional spectrum $E(\kappa)$, whereas standard hot-wire measurements yield the one-dimensional (1D) longitudinal spectrum $E_{11}(\kappa_1)$. In Appendix B we show that, under the assumption of isotropy, Eq. (11) yields the following relationship for the 1D longitudinal spectrum $E_{11}(\kappa, t)$:

$$\frac{E_{11}}{\epsilon^{2/3}L^{5/3}} = \frac{18}{55}C_k\kappa^{-5/3}[1 - 1.209c\kappa^{-2/3} + 0.407c^2\kappa^{-4/3}], \tag{13}$$

where $c = \frac{C_0 C_\epsilon^{2/3}}{3C_v}$. For $\mathrm{Re} \to \infty$ and $\kappa \to \infty$ Eq. (13) reduces to the standard prediction of the K41 theory for the longitudinal spectrum E_{11} [20].

Figures 4(a) and 4(b) present the results of one set of grid experiments conducted for this study (seven measurement stations with Re_λ varying from 129 to 95 when $C_\epsilon = \mathrm{const}$; see Appendix A for the full measurement details). We note that two grid sizes were tested at three inlet Reynolds numbers, adding up to six experimental cases, and all cases yielded qualitatively similar results. Figure 4(a) shows that the energy spectrum plots fall onto a single curve, when normalized according to the K41 theory. However, in accordance with the DNS results [see Fig. 1(b)] the spectral slope is somewhat flatter than $-5/3$. The normalized low-pass dissipation $\epsilon^>/\epsilon$ drops abruptly around $\kappa = 10$, which marks the onset of dissipative effects. In Fig. 4(b) we replot the energy spectra curves on lin-log axes. The compensation of Eq. (11) makes the energy spectrum a bit flatter, in accordance with the DNS results. Note that the factor $c = \frac{C_0 C_\epsilon^{2/3}}{3C_v}$ cannot be calculated unambiguously as in the DNS case, but we may still obtain an estimate. C_ϵ was measured to be roughly constant and equal to 1.1 (see Appendix A), while C_0 was taken to be 1.83, which corresponds to Saffman's invariant, as there are some indications that grid turbulence is of the Saffman type [22,23]. C_v could not be estimated from measurements and was taken to be unity, similar to the DNS case. It is believed that the coefficient C_v will not vary drastically between different cases, given that the small scales of turbulence are expected to exhibit universal properties [4,21]. The above values lead to $c = 0.65$ for our experiments.

To verify that the above experimental results are not configuration specific, data were extracted from the grid study of Comte-Bellot and Corrsin [24]. Figure 4(c) shows that also in that case the classical compensation does not produce a flat spectrum. Similar to the simulations and experiments, Comte-Bellot and Corrsin's data show that Eq. (13) produces a relatively flat compensated spectrum. We note that this data set includes three measurement locations downstream of the grid, where $C_\epsilon = 1.05$ and Re_λ varies between 60 and 72. Using Saffman's invariant, the measured value for $C_\epsilon = 1.05$, and $C_v = 1$, the coefficient c was estimated to be 0.63.

D. Generality of the theory

The proposed out-of-equilibrium extension of the K41 framework rests on three main conditions. First, the eddies considered are in quasiequilibrium. Second, there is a simple transportation of energy along the cascade. Third, the approach of equilibrium occurs in a balanced manner; that is, the interscale energy flux is self-preserving as it approaches its equilibrium value ϵ [see expression (4)]. We expect that the first two conditions are fulfilled in any unsteady cascade for wave numbers sufficiently separated from the integral length scale and the Kolmogorov microscale, i.e., as equilibrium is being approached. Regarding the third condition, the DNS data set suggests that it holds for cascades far from initial and boundary conditions. Indeed, the interscale energy flux becomes self-preserving only after a critical time has passed since the numerical forcing has stopped, while for earlier times it exhibits a transient behavior in which Π/ϵ is not constant in time [see Fig. 1(a)].

A natural question is then whether this self-preserving approach to equilibrium is exclusive to homogeneous turbulence or whether it is, more generally, an attractor state of all canonical turbulent flows far from initial and boundary conditions. This is left as an open question, as an exhaustive characterization of all canonical flow systems is beyond the scope of this work. However, we present the results of a particular case which hints that the proposed theory might be appropriate for flows with intense mean shear, far from initial conditions. Like for our turbulence grids, we used hot-wire anemometry to measure the evolving turbulence generated by two square bars side by side (see Appendix A for experimental details). This configuration was chosen as it produces extremely high values of mean shear, far larger than those in the wake of a single body [25]. Our results (see Fig. 5) show a trend similar to those of the grid turbulence, with the spectra not being flat when compensated by $5/3$, but becoming flatter when using the correction of expression (13). C_v and C_0 were assumed to

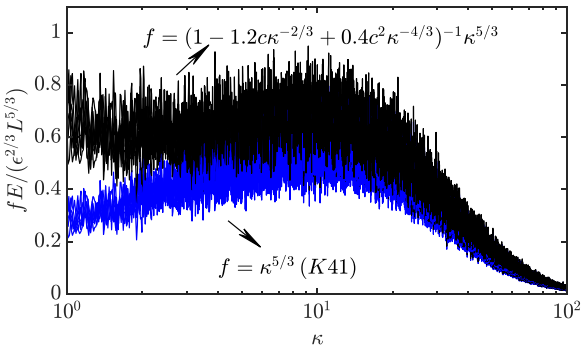

FIG. 5. Validation of expression (13) using energy spectra at seven measurement stations at the wake of two bars, side by side, with an estimated value of $c = 0.59$. f is as defined in the plot.

be unity and 1.83, respectively, similar to the grid turbulence case. C_ϵ varied depending on the measurement location but centered around 0.9 for the curves plotted (see Appendix A), while Re_λ varied from 150 to 120 for the curves plotted.

E. Comparison with previous theories

The revision of the K41 theory presented in this study is based on the balanced out-of-equilibrium behavior of large eddies and is thus not related to other corrections based on intermittency or time lag in the cascade [12,21,26,27]. As an example of an intermittency correction, we briefly discuss the OK62 theory of Oboukhov and Kolmogorov [12,13], but we note that other intermittency models are possible [26]. According to the OK62 model the spatial fluctuations in the turbulent energy dissipation rate at small scales are shown to render the $-5/3$ law slightly steeper, i.e., $\kappa^{-5/3-\mu/9}$, where $\mu \sim 0.2$ [27]. It was checked that this small difference in the exponent leaves the spectrum plots in Figs. 3(a) and 4(b) practically unaffected. In fact, it is known (see [28]) that the OK62 correction becomes significant only for larger moments of the velocity increment. This is in contrast to the current correction, which yields significant corrections for the power spectral density [see Figs. 3(b) and 4], where the slope becomes flatter (and not steeper as in OK62). Regarding the effect of time lag in the cascade, Pao [21] proposed a correction based on the speed V that energy is transferred across wave numbers, very similar to the current work. However, in Pao's theory V is used in conjunction with cascade equilibrium and yields corrections only for the dissipative scales of turbulence, leaving larger eddies, and thus the $-5/3$ law, unaffected (see Eq. (2.19) in [21]). We conclude that the above two types of corrections rest on different physical principles than the current theory, and in fact, we cannot think of any reason why they cannot apply simultaneously with the current correction.

V. CONCLUDING DISCUSSION

This work proposed a generalization of the K41 framework for unsteady cascades far from initial conditions and for finite wave numbers in quasiequilibrium. The current analysis was based on two main assumptions. The first is that far from initial conditions the interscale energy flux approaches its equilibrium value in a self-preserving manner. The second is that the quasi-isotropic wave numbers in question are characterized by a simple transportation of energy. Both of those assumptions were found to hold in the case of periodic box decaying turbulence far from initial conditions.

The above framework led to two main results. First, a correction to the $-5/3$ law was proposed for nonequilibrium and quasi-isotropic wave numbers in cascades far from initial conditions. Second, an equation which greatly resembles the dissipation equation of the $k-\epsilon$ model for homogeneous turbulence was derived. The above predictions were validated using data from numerical and laboratory experiments of homogeneous decaying turbulence.

When both the Reynolds number and wave number tend to infinity, Kolmogorov's equilibrium assumption is expected to be asymptotically fulfilled, even in highly unsteady turbulence cascades. This is consistent with the proposed theory: under these conditions the proposed modification becomes negligible, reducing to the K41 framework. However, even at very high Reynolds number, unsteady cascades will always contain a non-negligible range of scales, whose wave numbers are larger than the integral scale but of finite value, which will remain out of equilibrium. There, the $-5/3$ law will not be exact, and a self-preserving approach to equilibrium for the interscale energy flux will be necessary if the Kolmogorov dissipation law $\epsilon \propto K^{3/2}/L$ is to be derived, that is, so that the expression $\Pi \propto K^{3/2}/L$ (valid at $kL \approx 1$) can be used in conjunction with $\Pi \propto \epsilon$. We might therefore expect that the proposed theory is most suitable for those flows where the dissipation coefficient is found to be constant.

ACKNOWLEDGMENTS

This work was partly supported by an Imperial College London Junior Research Fellowship. I am grateful to Prof. C. Vassilicos for comments and discussions and for reading an early version of the manuscript, to Prof. S. Goto for providing me with the DNS data, and to Prof. M. Obligado for his help with the grid experiments and data processing. I am also grateful to LMFL and University of Lille, which provided me, during the Lille Turbulence Program 2020, with access to the LMFL's wind tunnel, which is part of the CONTRAERO regional platform.

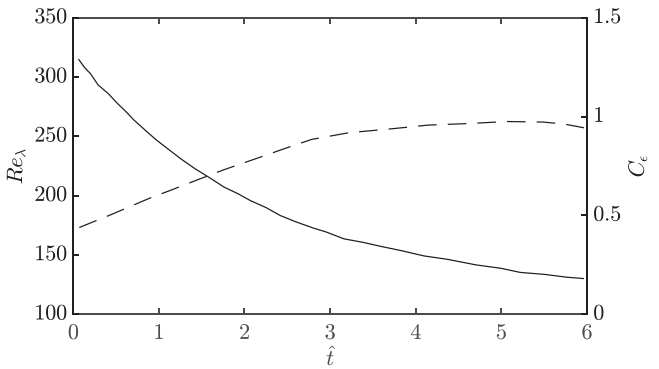

FIG. 6. Evolution of the Reynolds number (solid line) and dissipation coefficient (dashed line) as a function of the number of turnover times for the DNS data set used.

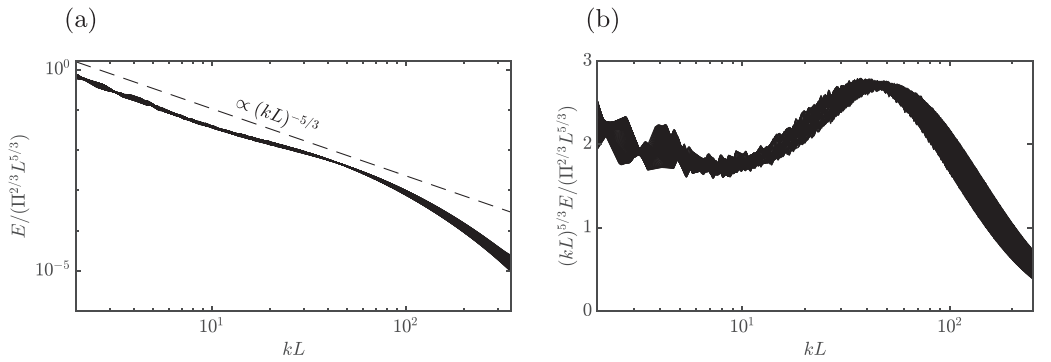

FIG. 7. Validation of the expression $\frac{E}{\Pi^{2/3}L^{5/3}} \propto \kappa^{-5/3}$ (note that $\kappa = kL$) for the interval where $C_\epsilon = \text{const}$ ($t > 3.5$). (a) Actual spectra and (b) compensated spectra with 5/3.

APPENDIX A: METHODOLOGY

1. Numerical experiments

For validation purposes, a data set of periodic box decaying turbulence is used, the details of which are presented in [8]. A forcing $f_s = (-\sin(k_f x)\cos(k_f y), \cos(k_f x)\sin(k_f y), 0)$ with $k_f = 4$ is imposed on the Navier-Stokes equations and is turned off at $t = t_0$ when dissipation is maximum, allowing the turbulence to decay. The simulation size was $N^3 = 2048^3$. The spatial resolution $k_{\max}\eta$ was slightly larger than that at t_0, while $k_{\max}\eta$ increased during decay. Figure 6 presents the evolution of the Reynolds number based on the Taylor microscale and of the dissipation coefficient as a function of the number of turnover times from the start of decay, defined as $\hat{t} = \int_0^t \frac{u}{L} dt$. Figure 7 validates the expression $\frac{E}{\Pi^{2/3}L^{5/3}} \propto \kappa^{-5/3}$ for the interval where $C_\epsilon = \text{const}$ ($t > 3.5$). For $\kappa > 2$ the previous expression collapses the energy spectrum, while the $-5/3$ scaling produces a relatively flat spectrum up to $\kappa = 20$.

We note that the plotted spectra demonstrate some fluctuations, evident in the linear axes plots [see, for instance, Fig. 3(a)]. These can be thought to be due to an insufficient convergence of the large eddy dynamics but also due to the proximity of the integral length scale, which might affect the collapse of the Kolmogorov theory.

For more information on the numerical details see Goto and Vassilicos [8].

2. Laboratory experiments

The experiments were conducted in the Lille wind tunnel at the Lille Fluid Mechanics Laboratory (LMFL). The wind tunnel has a measurement test section of 1×2 m^2 with a length of 21 m and provides for temperature regulation. For the free-stream velocities tested, the velocity fluctuations around the mean were measured to be 0.2% when the test section was empty. Hot-wire measurements were conducted using a single Pt-W 5 μm wire, 3 mm long, with a 1 mm sensing element. The probe was driven by a TSI IFA300 anemometer. The acquisition frequency was set to 50 kHz with a low-pass filter at 20 kHz. The acquisition time for each measurement location was 120 s. A systematic calibration of the probe was conducted at the beginning and at the end of each measurement campaign. It was checked that for all the data sets we had at least $k\eta = \frac{2\pi}{U} f\eta = 1$ (with η being the Kolmogorov scale, f being the Fourier frequency in hertz, and U being the local mean velocity).

For the grid measurements two planar grids were tested (hereafter G1 and G2). The G1 grid had a bar thickness of $t = 15$ mm and a mesh size of $M = 91$ mm. The G2 grid had a

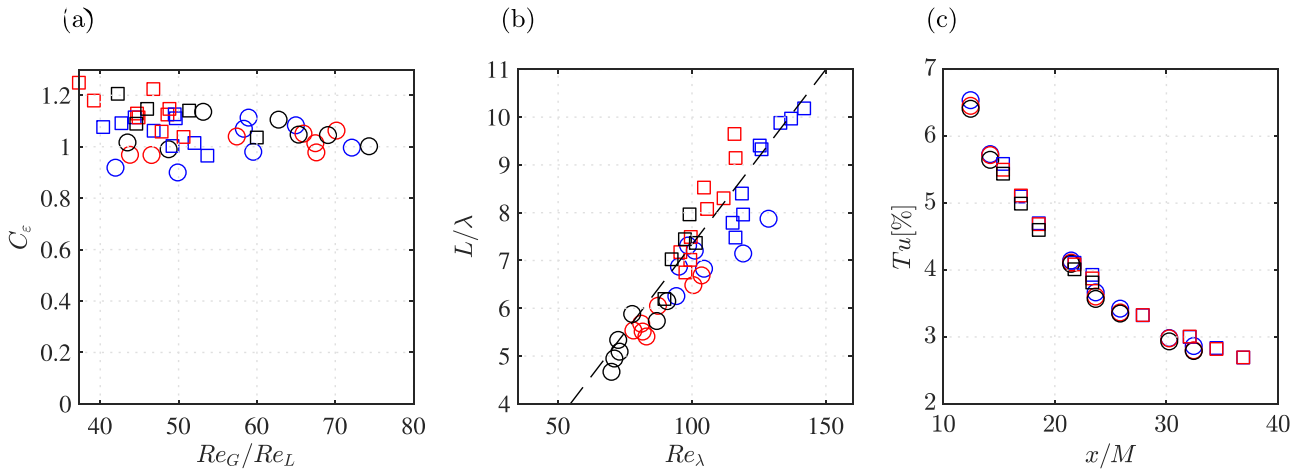

FIG. 8. (a) Measured dissipation coefficient, (b) L/λ, and (c) turbulence intensities for the G1 (circles) and G2 (squares) grids at inlet velocities 7, 5, and 4 ms^{-1} (blue, red, and black, respectively). The dashed line in (b) corresponds to $C_\epsilon Re_\lambda/15$ with $C_\epsilon = 1.1$.

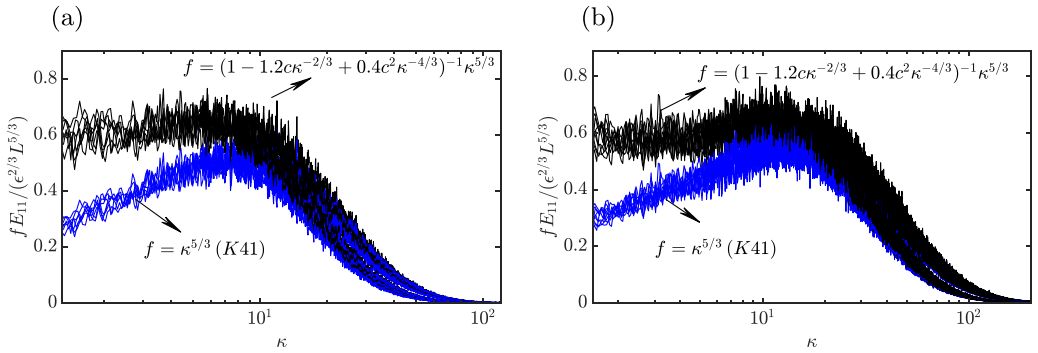

FIG. 9. K41 and current compensations for (a) the G1 grid at $\mathrm{Re}_G = 24\,300$ (seven measurement stations) and (b) the G2 grid at $\mathrm{Re}_G = 58\,300$ (nine measurement stations). The coefficient c was calculated to be equal to 0.65, as in Fig. 4(b) in the main text.

bar thickness of $t = 22$ mm and a mesh size of $M = 125$ mm. Both grids generated a tunnel blockage of 30%. Three inlet velocities were tested: 4, 5, and 7 m s^{-1} (in a few cases only the 5 and 7 m s^{-1} velocities were tested). The corresponding inlet Reynolds numbers based on the mesh size, Re_G, were 42 500, 30 300, and 24 300 for G1 and 58 300, 41 600, and 33 300 for G2. All measurements were conducted along the centerline of the grids.

To make sure that the data correspond to the region where C_ϵ remains constant, the measurements were conducted at distances larger than 12 mesh sizes from each grid [see Fig. 8(c) for the exact locations]. For smaller distances C_ϵ is known to increase as Re_λ^{-1} [11,16]. Figures 8(a) and 8(b) show that our measurements indeed lie in the region where C_ϵ is roughly constant, or, equivalently, $L/\lambda \propto \mathrm{Re}_\lambda$ [16], for both the G1 and G2 cases. The dissipation rate was estimated as $\epsilon = \int 15\nu k^2 E_{11} dk$, where $E_{11}(k)$ is the 1D power spectrum, calculated by means of the PWELCH algorithm. The longitudinal integral length scale was calculated using the zero-crossing methodology described in [29]. The Taylor microscale was calculated as $\lambda = \sqrt{15\nu\overline{u^2}/\epsilon}$. Figure 8(c) shows the evolution of the turbulence intensity $\sqrt{\overline{u^2}}/U$ as a function of the downstream distance from the grid, normalized with the mesh size. For both grids and at all three inlet Reynolds numbers the spectra showed a behavior almost identical to the ones plotted in Fig. 4(b) in the main text (which correspond to the G1 grid at $\mathrm{Re}_G = 42\,500$; see Fig. 9).

For the two-bar results shown in Fig. 5, two square bars with a thickness of $t_b = 25$ mm were positioned side by side, with a gap of 117 mm, spanning the whole height of the tunnel. The center of the gap coincided with the center of the tunnel. Two velocities were tested, 7 and 5 m s^{-1}. The measured turbulence intensities and dissipation coefficient are plotted in Fig. 10. In Fig. 5 only the seven farthest points of the high Reynolds number case (7 m s^{-1}) were used (i.e., the ones far from initial conditions). The hot-wire anemometry details were identical to those of the grid experiments described above.

We note that the experimental spectra, when plotted in linear scales, demonstrate some level of fluctuation. These can be thought to be connected to experimental errors, as they seem to be equally distributed in the small and large wave numbers of the cascade.

APPENDIX B: ONE-DIMENSIONAL ENERGY SPECTRUM

In the main text we derived the following expression for the three-dimensional spectrum of the inertial range:

$$\frac{E(\kappa,t)}{\epsilon(t)^{2/3}L(t)^{5/3}} \approx C_k[1 - c\kappa^{-2/3}]^2\kappa^{-5/3},$$

where C_k and c are constants. The three-dimensional spectrum E and the one-dimensional spectrum E_{11} are linked through the following expression, assuming isotropy (see Ref. [24]):

$$E(\kappa,t) = \frac{1}{2}\kappa^3\frac{\partial}{\partial\kappa}\left[\frac{1}{\kappa}\frac{\partial}{\partial\kappa}E_{11}(\kappa,t)\right],$$

where κ and κ_1 are used interchangeably given the spherically symmetric isotropic representation. By combining the above equations and integrating twice, we obtain the following expression for the one-dimensional longitudinal spectrum $E_{11}(\kappa,t)$:

$$\frac{E_{11}}{\epsilon^{2/3}L^{5/3}} = \frac{18}{55}C_k\kappa^{-5/3}[1 - 1.209c\kappa^{-2/3} + 0.407c^2\kappa^{-4/3}],$$

where $c = \frac{C_0 C_\epsilon^{2/3}}{3C_v}$. When $\mathrm{Re} \to \infty$ and $\kappa \to \infty$, the above equation reduces to the standard prediction of the K41 theory for the longitudinal spectrum E_{11} [20].

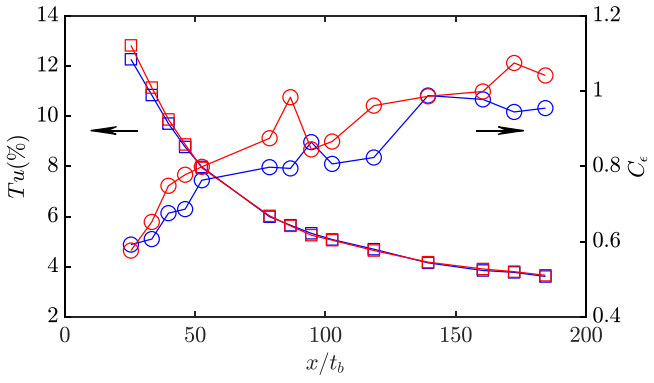

FIG. 10. Measured turbulence intensities (squares) and dissipation coefficient (circles) for the two-bar case as a function of downstream distance at inlet velocities of 7 and 5 m s^{-1} (blue and red, respectively). Only the last seven points of the high Re case are used for Fig. 5.

[1] A. N. Kolmogorov, Dissipation of energy in the locally isotropic turbulence, Dokl. Akad. Nauk SSSR A **32**, 16 (1941).
[2] A. N. Kolmogorov, On degeneration (decay) of isotropic turbulence in an incompressible viscous fluid, Dokl. Akad. Nauk SSSR A **31**, 538 (1941).
[3] A. N. Kolmogorov, The local structure of turbulence in incompressible viscous fluid for very large Reynolds numbers, Dokl. Akad. Nauk SSSR A **30**, 301 (1941).
[4] S. B. Pope, *Turbulent Flows* (Cambridge University Press, Cambridge, 2000).
[5] J. L. Lumley, Some comments on turbulence, Phys. Fluids **4**, 203 (1992).
[6] G. K. Batchelor, *The Theory of Homogeneous Turbulence* (Cambridge University Press, Cambridge, 1953).
[7] W. McComb and R. Fairhurst, The dimensionless dissipation rate and the Kolmogorov (1941) hypothesis of local stationarity in freely decaying isotropic turbulence, J. Math. Phys. **59**, 073103 (2018).
[8] S. Goto and J. C. Vassilicos, Unsteady turbulence cascades, Phys. Rev. E **94**, 053108 (2016).
[9] W. K. George, The self-preservation of turbulent flows and its relation to initial conditions and coherent structures, *Advances in Turbulence*, edited by W. K. George and R. E. A. Arndt (Hemisphere, 1989), pp. 39–72.
[10] W. K. George, The decay of homogeneous isotropic turbulence, Phys. Fluids **4**, 1492 (1992).
[11] J. C. Isaza, R. Salazar, and Z. Warhaft, On grid-generated turbulence in the near-and far field regions, J. Fluid Mech. **753**, 402 (2014).
[12] A. N. Kolmogorov, A refinement of previous hypotheses concerning the local structure of turbulence in a viscous incompressible fluid at high Reynolds number, J. Fluid Mech. **13**, 82 (1962).
[13] A. M. Oboukhov, Some specific features of atmospheric turbulence, J. Fluid Mech. **13**, 77 (1962).
[14] B. E. Launder and D. B. Spalding, The numerical computation of turbulent flows, Comput. Meth. Appl. Mech. Eng. **3**, 269 (1974).
[15] M. Obligado and J. C. Vassilicos, The non-equilibrium part of the inertial range in decaying homogeneous turbulence, Europhys. Lett. **127**, 64004 (2019).
[16] J. C. Vassilicos, Dissipation in turbulent flows, Annu. Rev. Fluid Mech. **47**, 95 (2015).
[17] S. R. Yoffe and W. D. McComb, Onset criteria for freely decaying isotropic turbulence, Phys. Rev. Fluids **3**, 104605 (2018).
[18] T. Ishihara, T. Gotoh, and Y. Kaneda, Study of high–Reynolds number isotropic turbulence by direct numerical simulation, Annu. Rev. Fluid Mech. **41**, 165 (2009).
[19] M. Meldi and J. C. Vassilicos, Analysis of Lundgren's matched asymptotic expansion approach to the Kármán-Howarth equation using the eddy damped quasinormal Markovian turbulence closure, Phys. Rev. Fluids **6**, 064602 (2021).
[20] K. R. Sreenivasan, On the universality of the Kolmogorov constant, Phys. Fluids **7**, 2778 (1995).
[21] Y. H. Pao, Structure of turbulent velocity and scalar fields at large wavenumbers, Phys. Fluids **8**, 1063 (1965).
[22] M. Sinhuber, E. Bodenschatz, and G. P. Bewley, Decay of Turbulence at High Reynolds Numbers, Phys. Rev. Lett. **114**, 034501 (2015).
[23] P.-Å. Krogstad and P. A. Davidson, Is grid turbulence Saffman turbulence?, J. Fluid Mech. **642**, 373 (2010).
[24] G. Comte-Bellot and S. Corrsin, Simple Eulerian time correlation of full-and narrow-band velocity signals in grid-generated, 'isotropic' turbulence, J. Fluid Mech. **48**, 273 (1971).
[25] J. Chen, C. Cuvier, J.-M. Foucaut, Y. Ostovan, and J. Vassilicos, A turbulence dissipation inhomogeneity scaling in the wake of two side-by-side square prisms, J. Fluid Mech. **924**, A4 (2021).
[26] U. Frisch, *Turbulence: The Legacy of A. N. Kolmogorov* (Cambridge University Press, Cambridge, England, 1995).
[27] P. A. Davidson, *Turbulence: An Introduction for Scientists and Engineers* (Oxford University Press, Oxford, 2015).
[28] L. P. Wang, S. Chen, J. G. Brasseur, and J. C. Wyngaard, Examination of hypotheses in the Kolmogorov refined turbulence theory through high-resolution simulations. Part 1. Velocity field, J. Fluid Mech. **309**, 113 (1996).
[29] D. O. Mora and M. Obligado, Estimating the integral length scale on turbulent flows from the zero crossings of the longitudinal velocity fluctuation, Exp. Fluids **61**, 199 (2020).